



كلية الهندسة - جامعة بغداد



اتحاد الجامعات العربية

Performance of Self-Compacted Reactive Powder Concrete Slab Under Harmonic Dynamic Loading

Mohammad Makki Abbass Bilal^{1,*}, and Safaa Adnan Mohamad²

¹ Department of Highway and Transportation Engineering, Al-Mustansiriyah University, Baghdad, Iraq

² Department of Highway and Transportation Engineering, Al-Mustansiriyah University, Baghdad, Iraq

* Corresponding author: Mohammad Makki Abbass Bilal

Published online: 31 March 2019

Abstract— Many types of loading the structure must sustain in addition to dead and live loads according to the function of structural element type that must be taken in analysis. Dynamic resistance to loading of reinforced concrete slabs using self-compact reactive powder concrete, with different boundary conditions at the sides in addition of static loading was studied. The reinforced concrete slabs were designed under static load according to ACI-318R-2014 and then the adequacy was checked under harmonic dynamic loading. The static loading consists of dead load and residential live load considering according to ASCE-07-2010. Modeling analysis was performed to determine the eigenvalues and eigenvectors values and then frequency response analyses of the slab by finite elements method that adopted for analysis. The results indicated that in case of self-compact reactive powder concrete rather than normal concrete gave deflection less and also there was a different result of deflection according the type of slab boundary condition supports.

Keywords— Finite element method, Self compact concrete, Reactive Powder concrete, Harmonic dynamic load.

1. Introduction

A harmonic analysis is used to determine the response of the structure under a steady-state sinusoidal (harmonic) loading at a given frequency. A harmonic or frequency-response analysis considers loading at one frequency only. Loads may be out-of-phase with one another, but the excitation is at a known frequency .

To improve concrete durability, strength and ductility with serviceability control largely carried out by using additives material to produce a concrete with special mechanical properties to resist various types of loading and reducible the dead load by reduced geometrical dimensions and increasing the strength. Using Reactive Powder Concrete (RPC) developed a composite material that allow with self-compact economic, benefit and build strong structural elements. Many researches discussed the advantages of high performance concrete as compared with the normal weight concrete due to better compressive and tensile strength with lower permeability. To increase the compressive strength of concrete, the coarse aggregate was removed so that there was no weakest link in the concrete.

Reactive powder concrete are composite materials consisting of cement, fine sand, powder and silica fume with or without steel reinforcement. Self-Compact Reactive Powder Concrete (SCRPC) has advantages that provide high ductility, high toughness, with improvement in workability, and high residual strengths after the initiation of the first crack. Experiences in the development of Ultra High Performance Concrete found very high flow ability in concrete with low water powder ratio. Because of the high viscosity of the cement paste, compaction was necessary. Falati, (1999) [1] investigated the dynamical behavior of reinforced concrete (RC) slabs on non-structural components by used pre-stressing reinforcement force to increase the capacity of slabs by increasing the natural frequency and decreased damping. Ma and Dietz (2002) [2] investigated UH performance self-compacting concrete by adding coarse aggregate and reached a compressive strength "150 MPa" and showed that very good workability. Barros et al. (2008) [3], evaluated the contribution of steel fiber reinforcement for the moment capacity of slab. The twelve slabs were checked under four points load with different parameters, steel fiber, steel reinforcement and strip loading. The results from

experiment were checked by numerical analysis and showed close. Ragab (2013) [4] studied punching shear of RC slab in presence of steel fiber and self – compact concrete. Experiment tests and to check the results value from tests, numerical analysis approach was adopted (FEM) with nonlinear analysis was modeled and analyzed and the results closed. Saaid et al. (2013) [5], investigated flexural behavior of concrete slab in presence of steel fibers and self-compacting concrete. Numerical analysis was used to check the experimental results by finite elements method (FEM) and showed that close values. The experimental results showed that there are increased in flexural resistance in case of presence of steel fiber as compared with the normal weight concrete slab. Rich (2014) [6], investigated the self-compacting concrete in situ to create optimum solution of concrete in site. The results indicated that self-compact concrete reduce construction time of slabs up to (73%) and reduce the total cost. Aboshio and Ye (2015) [7], studied the effects of static and dynamic analysis on RC slabs. Linear analysis was adopted and discussed the cost wise effects of slabs response. Bijan O Aalami (2008) [8], studied the behavior of reinforced concrete floor-spandrel beams using (FEM).

A verification of the (FEM) models under static loading was established by comparing the numerical results with the available experimental results and a very good agreement was obtained. In present paper, mechanical properties enhanced by using SCRPC to resists static and dynamical loading that applied directly on RC slabs and compared the results with different boundary conditions of slabs using finite element analysis.

2. Objective of Study

In present paper, evaluation of self-compacted reactive powder concrete slab under harmonic dynamic loading was examined and discussed. Different parameters were adopted such as boundary conditions at the sides of reinforced concrete slab in addition of static and dynamic loading by analytical and finite elements approach.

3. Dynamical analysis - Harmonic

Frequency-domain analysis is based upon the dynamical response of the structure to harmonically varying load. At each frequency, the loading varies with time as sine and cosine functions. Steady-state analysis computes the deterministic response at each requested frequency. The loading may have components at acting different phase angles. The equations used to find the theoretical conclusion to applied in the program

Harmonic loading is of the form Equation.1:

$$r(t) = P_0 \cos(\omega t) + P_{90} \sin(\omega t) \quad (1)$$

where (ω) is the circular frequency of the excitation [9]. This loading is assumed to exist for all times, so that transient components of the response have vanished, so, steady-state conditions have been achieved. The spatial

loading consists of two parts: the in-phase component P_0 , and the 90° out-of-phase component P_{90} . The spatial distributions do not vary as a function of time. The equilibrium equation for the structural system is Equation.2[9]:

$$Mu''(t) + Cu'(t) + Ku(t) = P_0 \cos(\omega t) + P_{90} \sin(\omega t) \quad (2)$$

Where (K) is the stiffness matrix, (C) is the viscous damping matrix, (M) is the diagonal mass matrix, and (u''), (u'), and (u) are the node accelerations velocities, and displacements, respectively.

Equation .2, rewrite transfer to the complex form, so that the applied loading expressed as Equation.3[9]:

$$\bar{r}(t) = \bar{P} e^{i\omega t} = \bar{P} (\cos(\omega t) + i \sin(\omega t)) \quad (3)$$

The real cosine term represents the in-phase component, and the imaginary sine term represents the 90° out-of-phase component. The steady-state solution of this equation requires that the node displacements are of the same form Equation .4, so that the equation of motion after rearranged becomes as Equation .5.

$$\bar{u}(t) = \bar{a} e^{i\omega t} = \bar{a} (\cos(\omega t) + i \sin(\omega t)) \quad (4)$$

$$[K + i\omega C - \omega^2 M] \bar{a} = \bar{P} \quad (5)$$

And the complex impedance matrix is from Equation. 6:

$$\bar{K} = K - \omega^2 M + i\omega C \quad (6)$$

The real part represents stiffness and inertial effects, and the imaginary part represents damping effects. The Equation.7 is the equation of motion.

$$\bar{K}(\omega) \bar{a}(\omega) = \bar{P}(\omega) \quad (7)$$

In case of frequency domain specify a hysteretic (displacement-based) damping matrix (D) rather than a viscous (velocity-based) damping matrix (C). These are related as Equation.8:

$$D = \omega C \quad (8)$$

Hysteretic damping specified as a function of frequency, i.e., $D = D(\omega)$, and there is no restriction imposed on the value at $\omega = 0$. Using hysteretic damping, the complex impedance matrix, Equation.9.

$$\bar{K}(\omega) = K(\omega) - \omega^2 M + iD(\omega) \quad (9)$$

In present paper, for each Steady-state load case, damping coefficients that apply to the structure as a whole. The damping matrix is calculated as a linear combination of the stiffness matrix scaled by a coefficient, (d_k), and the mass matrix scaled by a second coefficient, (d_m). The case

studied in present work, ($d_M = 0$) and only (d_K), is used. Thus, the damping matrix form Equation.10:

$$D(\omega) = d_k(\omega)K + d_M(\omega)M \quad (10)$$

Assuming that ($d_M = 0$) and ($d_K(\omega)$) to linearly increase with frequency, this is equivalent to viscous damping and the value of $d_K(\omega) = 2d(\omega)$, where $d(\omega)$ is the modal damping ratio with constant "5%" modal damping for all modes, so that the equivalent hysteretic damping value is a constant ($d_K(\omega) = 0.10$), for each mode, this leads to approximately the same level of response at resonance.

Frequency domains analyses are performed at discrete frequency steps. For a Steady-state load case, the frequencies from Equation .11, the frequency step adopt here is (1 Hz):

$$f_1, f_1 + \Delta f, f_1 + 2\Delta f + \dots \quad (11)$$

Where, $\Delta f = (f_2 - f_1)/n$, all frequencies calculated in a specified modal load case. Only frequencies that fall within the frequency range (f_1 to f_2), will be used in present study. The modal frequencies analysis and their fractional deviations adopted in present work to capture resonant behavior in the structure. Any set of equally-spaced frequencies could easily skip over the most significant response in a given frequency range.

4. Theoretical analysis

A machine is assumed with a spinning fly wheel that has an eccentric mass. The mass is (m), and the center of mass is eccentric by an amount (e). The magnitude of the force from the eccentric mass that acts on the center of rotation and the applied load is given by Equation.12[10]:

$$F = em \omega^2 S_f \quad (12)$$

where, (F), dynamic force amplitude (zero-to-peak) in (Newton), (m), rotating mass in (kg); (e), mass eccentricity, in (mm), (ω), circular operating frequency of the machine (rad/s), and (S_f), service factor, used to account for increased unbalance during the service life of the machine, generally greater than or equal to 2. The maximum allowable mass eccentricity given by Equation (13) [10]:

$$f_j(\omega) = \omega^2 \quad (13)$$

(f_0) is the operating speed, ($\text{rpm} \leq 25,000 \text{ rpm}$), the steady-state function, which varies in Equation 14[10], The response at phase angle (θ_0), primarily represents the behavior due to horizontal.

$$U = m_1 r = M_1 e \quad (14)$$

The rotor is symmetrical except for the unbalanced m_1 at radius from Equation.15[10], Fig. 1:

$$e = \frac{6.35}{f_0} \quad (15)$$

where, (M_1) is the rotor mass, (m_1) unbalanced mass, (C_1) center of mass, (e) displacement of mass center, (r) distance from center of rotor to the center of gravity of unbalanced mass (m_1), (F_1) force due to unbalanced, (U) rotor unbalanced and (N) rotor speed (rpm). According to American Petroleum.

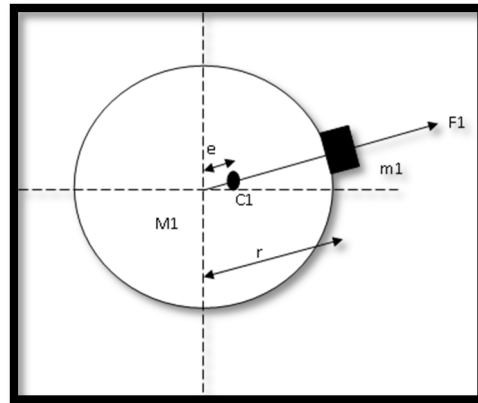


Figure 1: rotor mass with the bearing centers scheme.

Institute (API – 610) [10], the tolerance (T) in (kg) given by Equation.16 :

$$y = k \frac{a^4 q}{E h^3} \quad (16)$$

Where, W , rotor weight in (kg), N , speed in (rpm) according to the International Standard Organization (ISO – 1940) [11], the balance tolerance is given by Equation.17:

$$U_{per} = \frac{9.54 G \text{ mass}}{N} \quad (17)$$

Where, (U_{per}) is the permissible balance tolerance, (G) number depends on rotor, (mass) in grams and (N) in rpm.

5. Finite element simulation

The finite element analysis (FEA) used to simulate the actual slabs by structure composed of elements connected together at a finite number of nodes. The displacement at any point within the element can be related to the nodal placements. ETABS [9] and after that checked by ANSYS [12] software's to simulate the slabs that subjected to static with model dynamic analysis by using ETABS and dynamic harmonic loading by using ANSYS. The numerical simulation relies on the suitable selection of elements type SOLID65 element is used for concrete, LINK180 for steel reinforcement in ANSYS discrete model so that the concrete nodes are similar for steel reinforcement, and shell type in ETABS for slab), number,

proper material models, suitable boundary condition simulation, convergence criteria and solution method.

Table 1: Results of ratios for modal analysis (Pin/Fixed).

Mode	Circular frequency ratio	Frequency ratio	Eigenvalues ratio
1	0.997348959	0.99735	0.994705
2	0.997348959	0.99735	0.994705
3	0.991851354	0.991852	0.983769
4	0.996115899	0.996116	0.992247
5	0.999329943	0.99933	0.99866
6	0.992162196	0.992163	0.984386
7	0.992162196	0.992163	0.984386
8	0.997165755	0.997166	0.99434
9	0.99771895	0.997718	0.995443
10	0.99771895	0.997718	0.995443
11	0.993338915	0.993339	0.986722
12	0.993570102	0.993571	0.987182

Compressive strength and modulus of elasticity for ordinary concrete (25 MPa) and (23500 MPa) respectively, Poison's ratio for concrete and steel are (0.15) and (0.30) respectively. Slab dimensions (4x4m) with (150 mm) thickness and reinforced by steel reinforcement with diameter (12 mm) at (150 mm) center to center designed based on the ACI-318R-14 [13] code under dead load and live load according to ASCE-07-2010 [14] as residential building (1.92 kN/m²), mass of concrete and reinforcement needed in dynamic analysis that considered based on the geometry dimensions of concrete slab and diameter of reinforcement with density (25 kN/m³) and (78.5 kN/m³) respectively. Fig. 2 shows the slab with pin condition surrounding the perimeter while Fig.3 shows the fixed boundary in both figures the node position in the center of the slab and the deflection results as static and dynamic at the bottom face of the slabs. Mechanical properties are listed in Table 3 which represent the SCRPC mechanical properties and there are differences in values as compared with the normal weight concrete mentioned above.

Modal analysis by using ETABS to specify the frequencies of two types of slab that listed in Table 1 as frequency ratio (Pin/Fixed).

The full performance of RC slabs that gives maximum deflection at center of each boundary condition has shown in Fig. 10 to 15 in case of normal weight concrete. Results are compare with the empirical formula that adopted by many researchers from Equation.18 lists in Table 2.

$$T = \frac{6350W}{N} \quad (18)$$

Where (k), equal to (0.0143) or (0.0457) [15] for fixed or pinned boundary supports conditions respectively. Table 2 listed the results value for pinned and fixed conditions and the numerical equation results Equation 18.

Table 2: Deflections in bottom central slab – normal concrete.

Deflection (mm)	Pin ended	Fixed ended
ETABS	1.540	0.490
ANSYS	1.458	0.4569
Empirical formula Equation (17)	1.586	0.496

Table 3: Mechanical properties of self-compacted reactive powder concrete [15].

Mark	% Silica fume	% Fiber	fc' (MPa)	Split tensile (MPa)	Modulus of rupture (MPa)	Modulus of Elasticity (MPa)
A	15	2	120	17.2	19	47810
B	15	0	75	5.3	5.4	38600

6. Self-compacted reactive powder concrete (SCRPC)

The special type of concrete mixture characterized (self-compact), high resistance to segregation, that can be cast without compaction or vibration as manual or mechanical. The Self-Compact Concrete (SCC) slips freely without need to compact that distributed and surrounding around the steel reinforcement within mold uniformly. The main advantages of (SCC) not for structural requirements only but to shortening construction time, eliminate noise and to ensure that the compaction for concrete enough to cast. The presence of silica fume enhances the behavior of concrete to manufacture self-leveling concretes with great cohesion of the fresh mix. Also, the presence of steel fiber very useful to produce a new concrete that named Self-compact Reactive Powder Concrete (SCRPC). Data listed in Table 3 was selected from previous work to make it as input data for present paper [16].

Deflection counters for two types of slabs shown in Figs. 16 to 23 that were simulated in ETABS and ANSYS. Table 4 lists the central deflection for SCRPC in case of static loading.

7. Harmonic loading

The case adopted here is the rotate machine with constant speed in top of the slab that designed before under static loading only. The machine considered is mounted on a structure, the steady-state response of the structure to the machine running at any speed in the range from 0 to 50Hz (3000 rpm). According to ACI – 351.3R – 04, Table 3 [17], balance quality grades for selected groups of representative rigid rotors, product of ($\epsilon\omega$), (mm/s), (G1) is (1 mm/s) was selected, rotor mass (250 kg), radius (420 mm) and speed (3000 rpm). By using equations mentioned above according to API – 610, the tolerance is (529 g/mm), according to ISO – 1940 is (795), therefor the value of (ϵ) is (3.18 g.mm/kg). The permissible unbalanced mass is

(1.89) and based on API – 610 is (1.25). Based on ACI – 351.3R – 04 [4], typical live loads vary from (2.9 kPa) for personnel to as much as (7.2 kPa) for maintenance equipment and materials, the load adopted in present work was (7.0 kPa), and the calculated dynamic force amplitude (Fo) is (200 N). Figs.24 to 29 represent the full performance of all models of SCRPC under harmonic loading. The curves wavering and the deflection at central bottom slab vary with respect to frequency values ranging from (0-50 Hz). The maximum deflection and corresponding frequency are listed in Table 4 for all types of slab and concrete. Figs. (30 and 31) represent the central deflection with frequencies for all concrete types and slab boundary conditions.

Table 4: Maximum deflection for all types of slab and concrete models under harmonic loading.

Mark	Concrete type	Maximum deflection (mm)	Frequency (Hz)	Deflection for same frequency of normal concrete
Pinned slab	Normal concrete	2.11E-04	1	2.11E-04
	SCRPC - A	1.95E-04	2	1.95E-04
	SCRPC - B	3.99E-04	4	1.96E-04
Fixed slab	Normal concrete	1.66E-02	8	1.66E-02
	SCRPC - A	4.86E-04	29	6.95E-07
	SCRPC - B	5.79E-04	3	1.78E-06

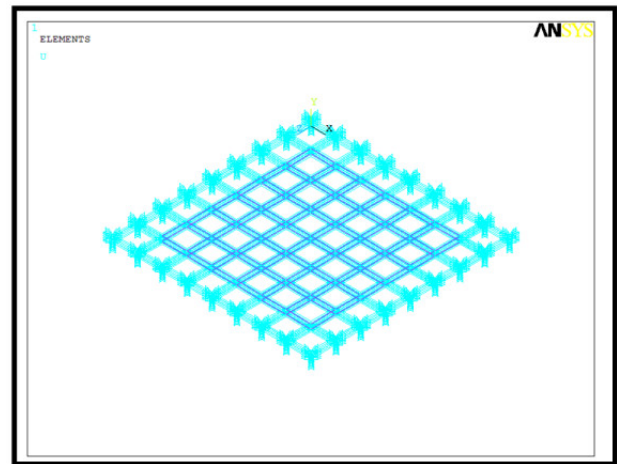


Figure 3: Fixed slab.

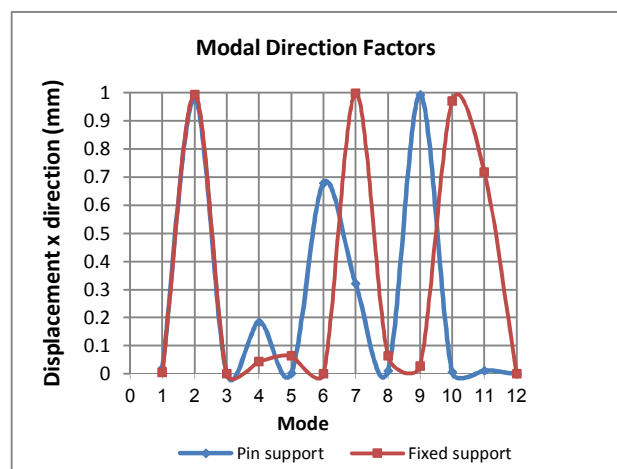


Figure 4: Modal direction factor –Displacement X direction.

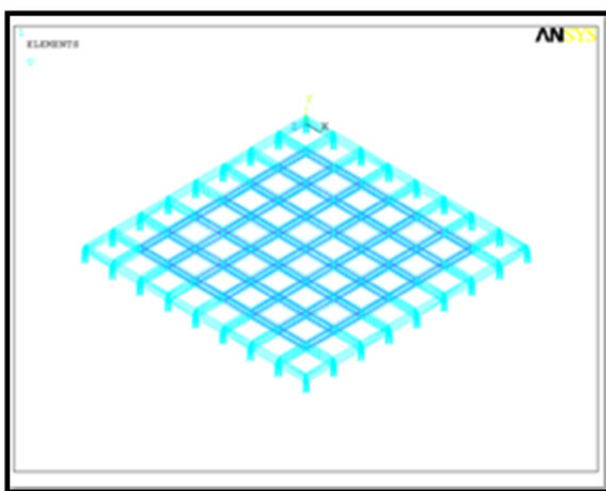


Figure 2: Pinned slab.

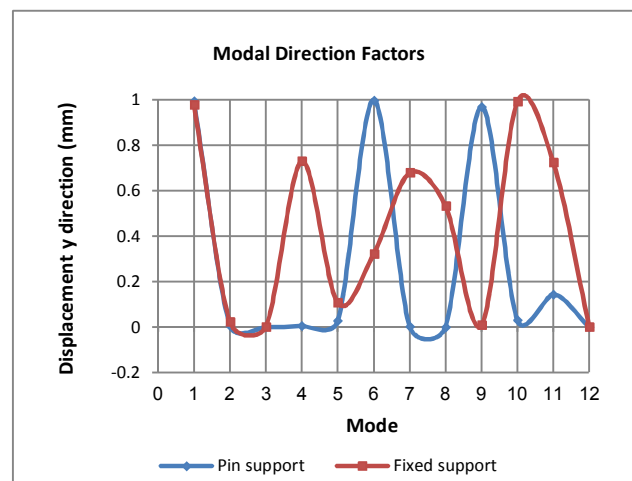


Figure 5: Modal direction factor –Displacement Y direction.

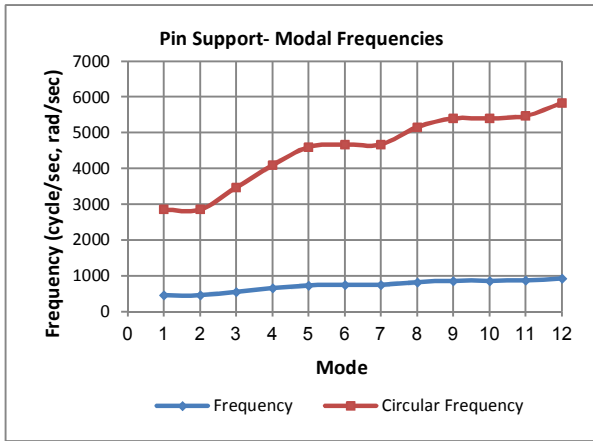


Figure 6: Modal analysis –Frequency and circular frequency for pinned slab.

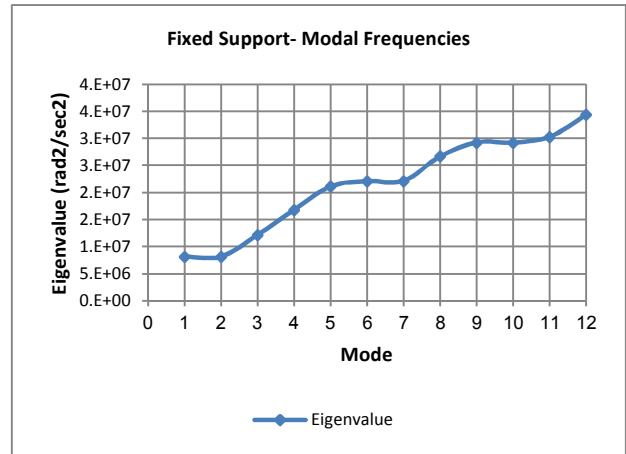


Figure 9: Modal analysis –Eigenvalues with mode for fixed slab.

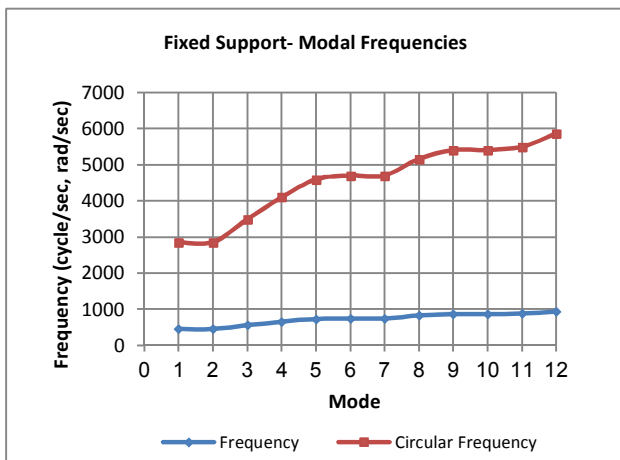


Figure 7: Modal analysis –Frequency and circular frequency for fixed slab.

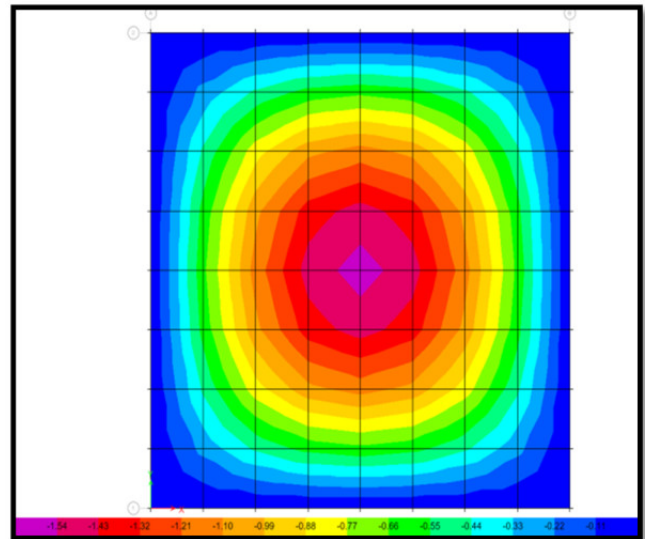


Figure 10: Deflection contour – pinned slab – normal concrete – ETABS.

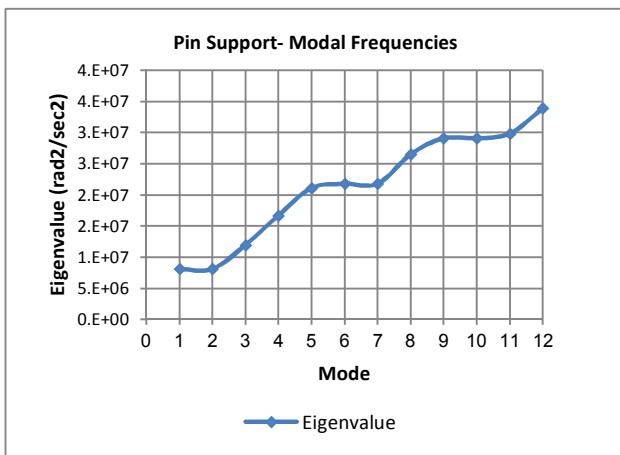


Figure 8: Modal analysis –Eigenvalues with mode for pinned slab.

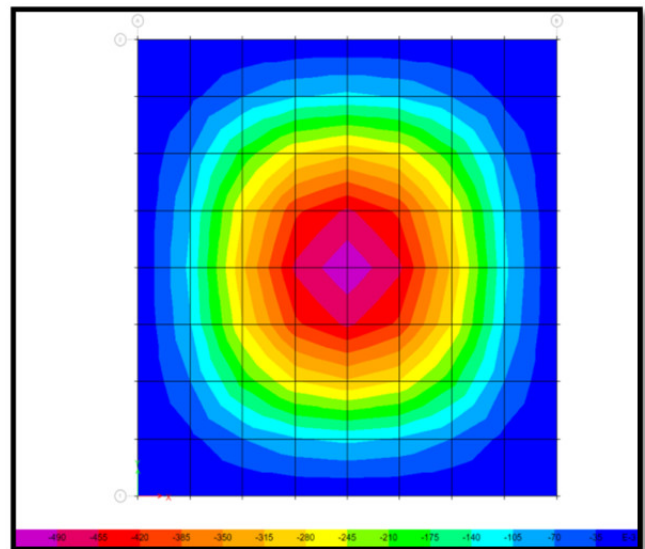


Figure 11: Deflection contour – fixed slab - normal concrete – ETABS.

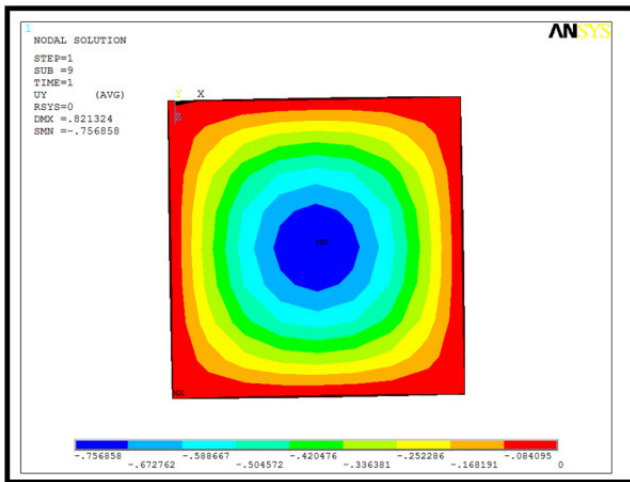


Figure 12: Deflection contour – pinned slab – normal concrete – ANSYS

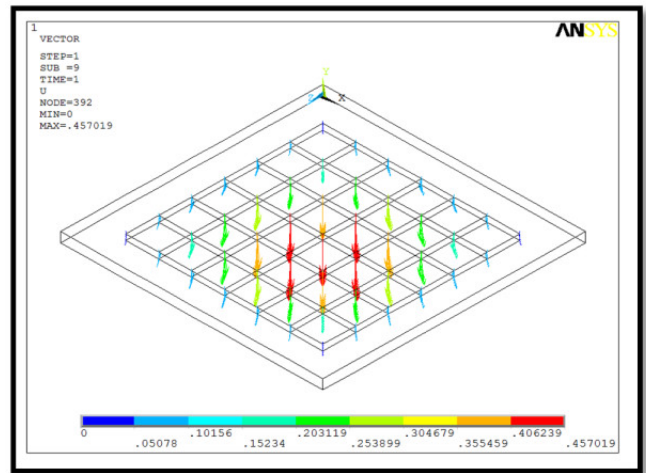


Figure 15: Deflection vector – fixed slab – normal concrete – ANSYS

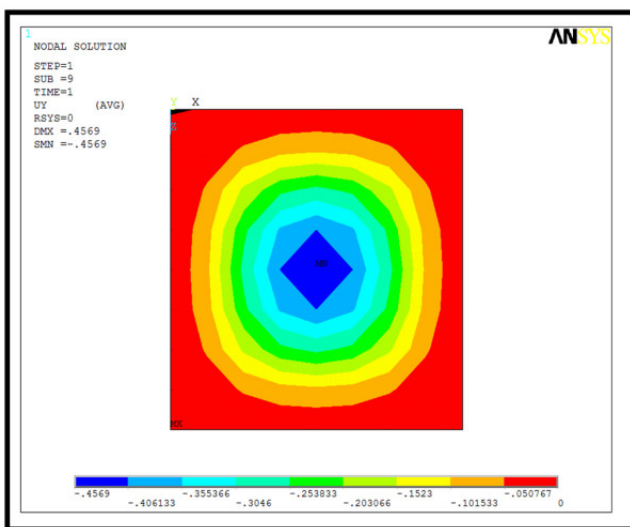


Figure 13: Deflection contour – fixed slab - normal concrete – ANSYS.

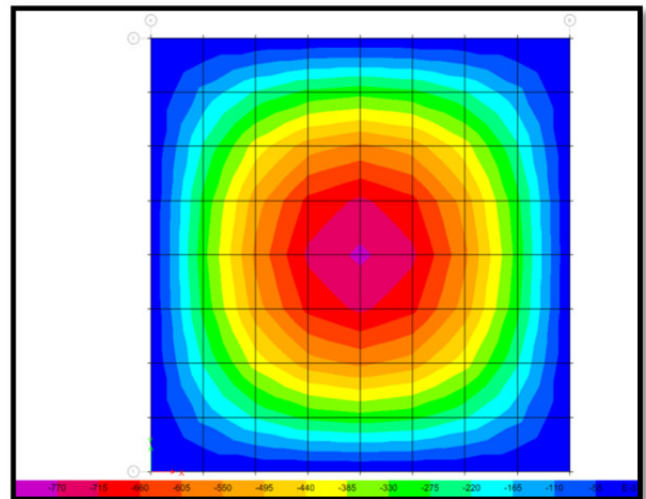


Figure 16: Deflection contour – pinned slab – A – ETABS.

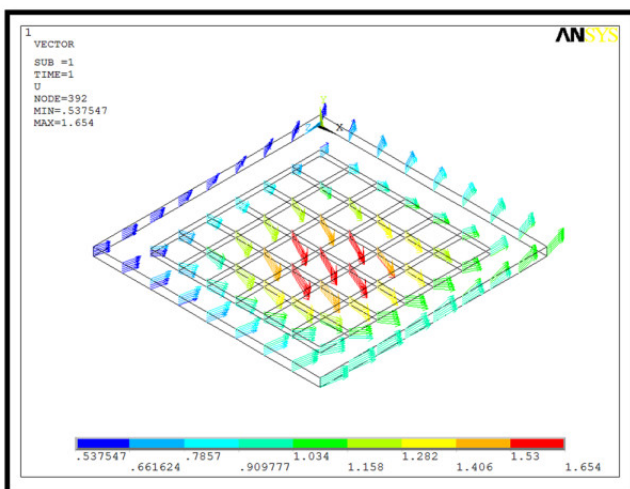


Figure 14: Deflection vector – pinned slab – normal concrete – ANSYS.

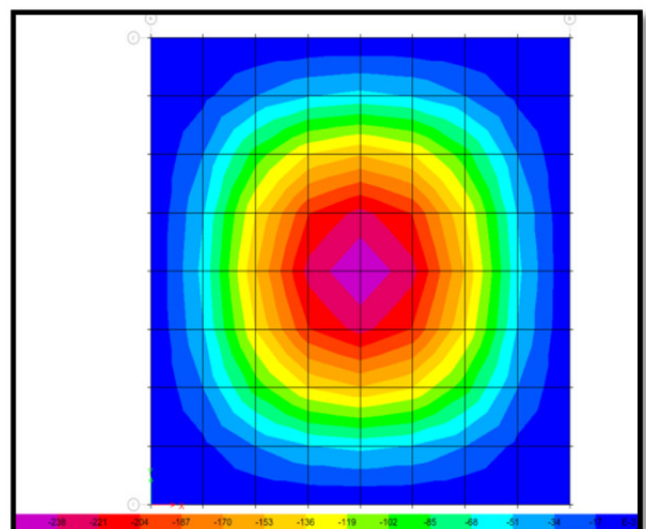


Figure 17: Deflection contour – fixed slab – A – ETABS.

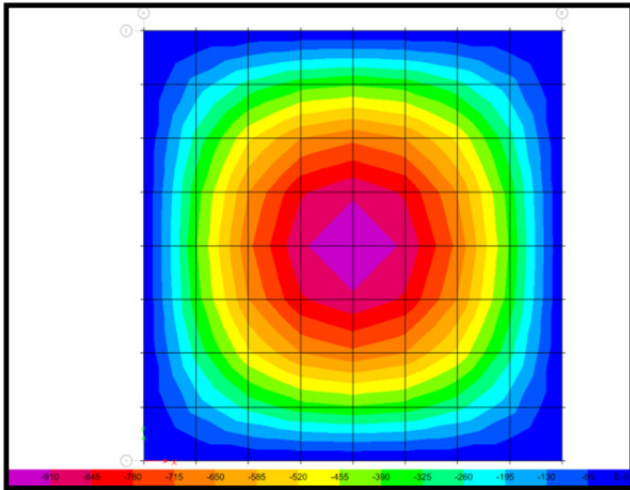


Figure 18: Deflection contour – pinned slab – B – ETABS

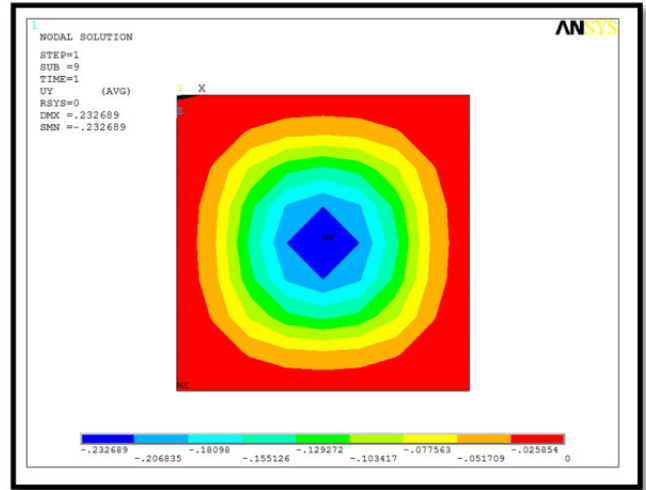


Figure 21: Deflection contour – fixed slab – A – ANSYS.

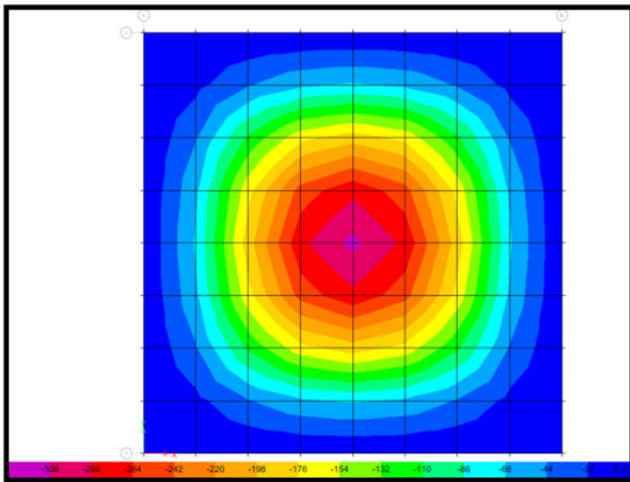


Figure 19: Deflection contour – fixed slab – B – ETABS.

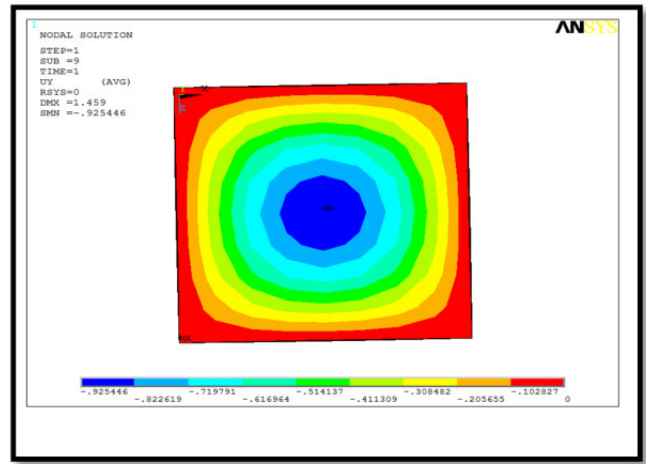


Figure 22: Deflection contour – pinned slab – B – ANSYS.

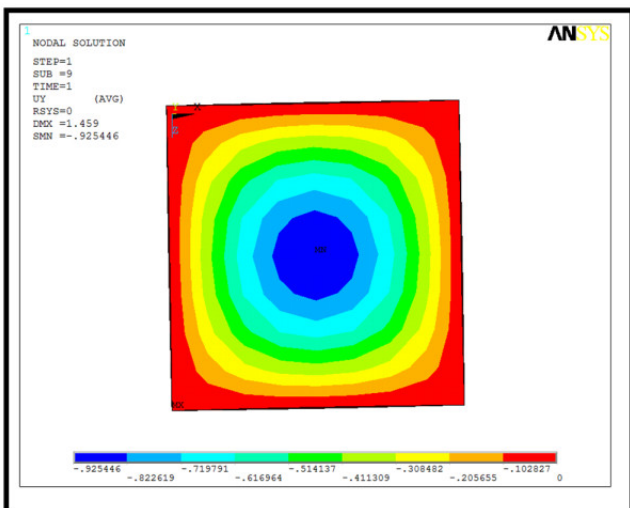


Figure 20: Deflection contour – pinned slab – A – ANSYS.

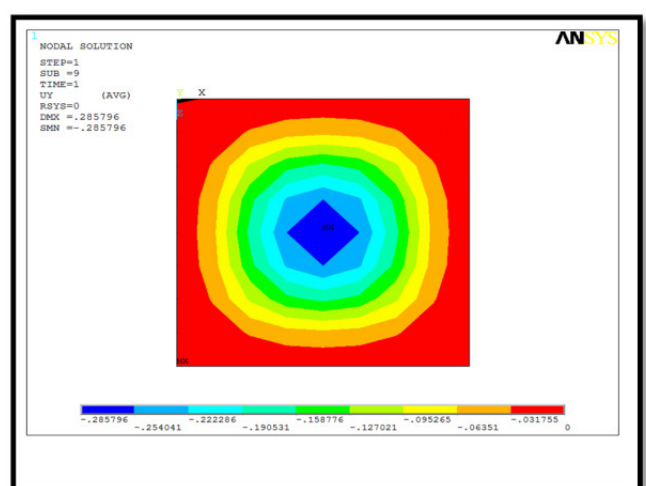


Figure 23: Deflection contour – fixed slab – B – ANSYS.

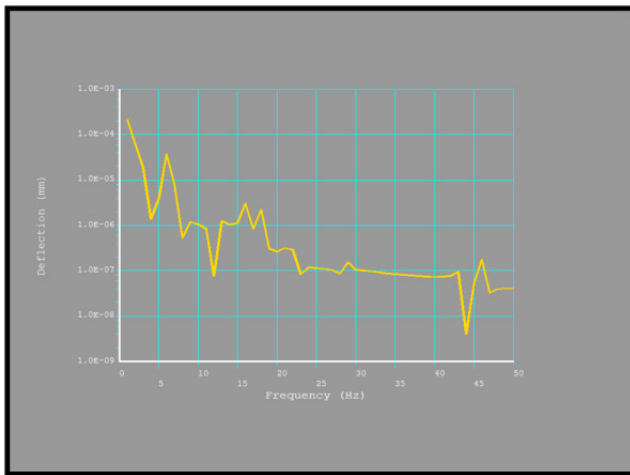


Figure 24: Deflection – Frequency- pinned slab – normal concrete – ANSYS.

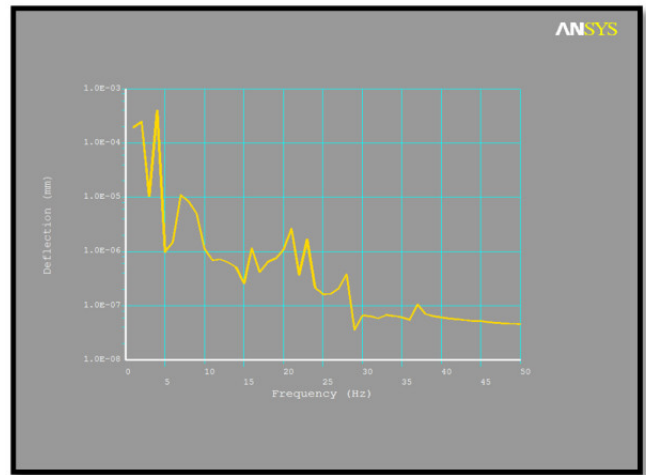


Figure 27: Deflection – Frequency- pinned slab – SCRPC - B – ANSYS.

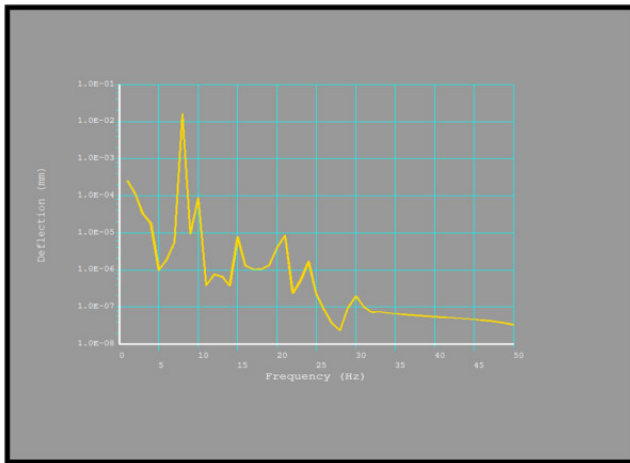


Figure 25: Deflection – Frequency- fixed slab – normal concrete – ANSYS.

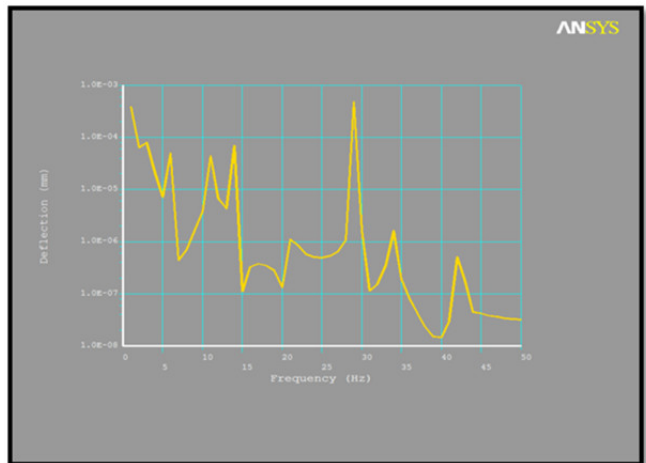


Figure 28: Deflection – Frequency- fixed slab – SCRPC - A – ANSYS.

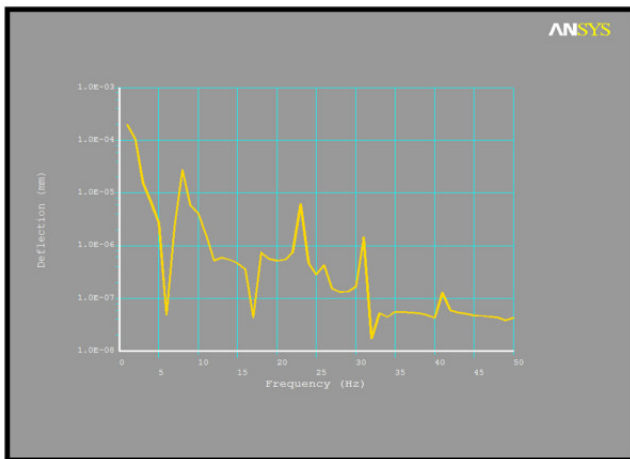


Figure 26: Deflection – Frequency- pinned slab – SCRPC - A – ANSYS.

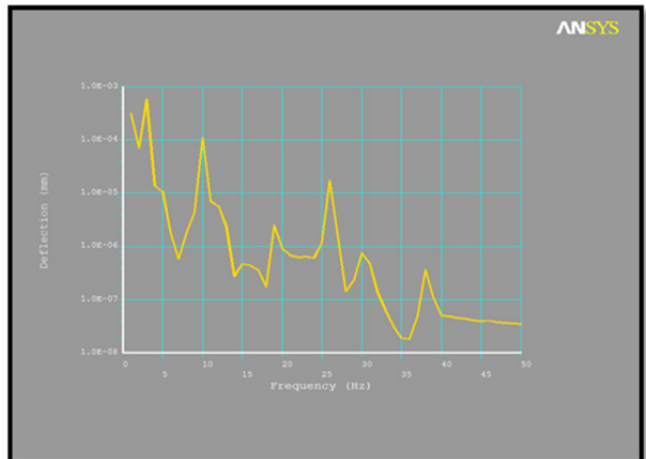


Figure 29: Deflection – Frequency- fixed slab – SCRPC - B – ANSYS.

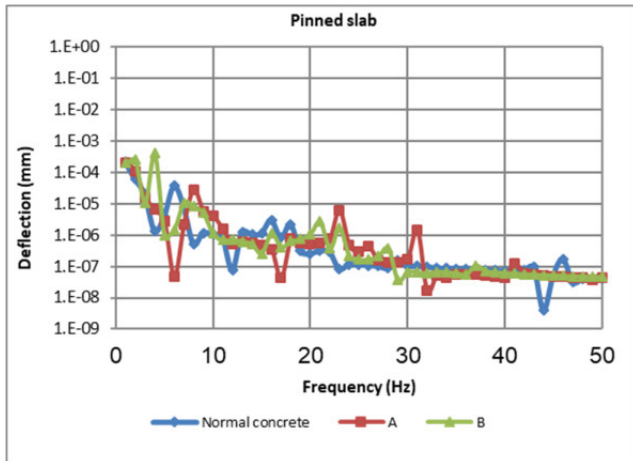


Figure 30: Deflection – Frequency- pinned slabs – SCRPC – all models.

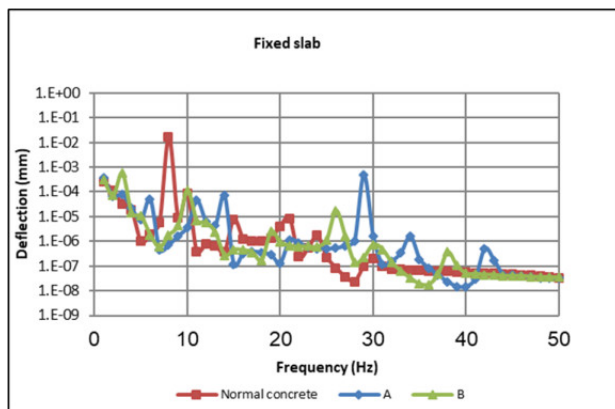


Figure 31: Deflection – Frequency- fixed slabs – SCRPC – all models.

From the results there was enhancement and improvement in the performance of concrete in case of SCRPC as compared with normal concrete as deflection when the slab subjected to harmonic loading. Table (5) listed deflections – Frequency, deflection reduced in case of concrete A and B if compared for same frequency, also concrete type A less than type B because of presence of fiber. Frequencies that cause maximum deflection not equal the natural frequency of match the frequencies from Table (1), so that no resonance will occur.

Table (5) showed that the deflection of slab that contain type A and B less the normal concrete 7.5% and 7% for pinned slab, and, 98%, for fixed slab.

8. Conclusion

Reinforced concrete slabs manufactured from normal and SCRPC with different boundary conditions support subjected to static and dynamic loading was studied. The following points were concluded from the study:

1. From the equations found that the imbalance in rotating machinery is the common source of harmonic excitation due to unsatisfactory balancing of rotating

parts in practice the mass centroid of rotating part does not coincide with center of rotation.

2. Finite elements simulation deflection results by ETABS and ANSYS software give closed results. The little difference between the results are 5.3% for pin ended, 6.7% for fixed ended because of properties of elements in each software and accuracy.
3. The deflection values for normal concrete within range of serviceability, the deflection acceptable based on ACI – 318 – 2014 is (L/240) around (16.67 mm).
4. Using SCRPC makes increase in mechanical properties of concrete as compressive strength and modulus of elasticity and then reflect to reducible in deflection about 37% and 51% for pinned slab in case of A and B, also in case of fixed slab 48% and 50% for fixed slab in case of A and B as compared with the normal concrete results.
5. There was enhancement and improvement in the performance of concrete in case of SCRPC as compared with normal concrete as deflection when the slab subjected to harmonic loading.
6. Frequency of slab changed as the mechanical properties changes because of the internal resistance of concrete rely on mechanical properties (modulus of elasticity).
7. Fixed slab gives less deflection under static and dynamic loading because of zero slop at supports make restraint so that the resistance increased.
8. Deflections due to harmonic loading are less than that from static because of the frequency ranged for this type of loading hit this structural geometry that adopted not cause damaged more than static loading deflection, but the important that the frequency and then after time caused that deflection not equals for all types.

References

- [1] Aaron Aboshio and Jianqioa Ye, "Reinforced concrete slab under static and dynamic loadings", World Academy of Science, Engineering and Technology, International Journal of Civil, Environmental, Structural, Construction and Architectural Engineering Vol.9, No.12, 2015, pp. 1410-1415.
- [2] ACI Committee 318, "Building Code Requirements for Structural Concrete", (ACI 318-14) and Commentary (ACI 318R-14), American Concrete Institute.
- [3] ACI Committee 351.3R, "Foundations for Dynamic Equipment ", (ACI 351.3R -04), Reported by ACI Committee 351, American Concrete Institute.
- [4] American Society of Civil Engineers, "Minimum Design Loads for Buildings and Other Structures", ASCE/SEI 7-10.

- [5] American Petroleum Institute, API standard – 610, eleventh edition, September 2010.
- [6] Anis A. Mohamad Ali and Rasha M. Shareef Salman, "Parametric study of the behavior of reinforced concrete spandrel –floor beams", International Journal of Innovative Research in Science, Engineering and Technology, Vol. 4, Issue 8, August 2015, pp. 6856-6863.
- [7] ANSYS Software, User's Manual Revision Inc., Multiphysics, Release 15, 2015.
- [8] Bijan O Aalami, "Deflection of concrete floor systems for serviceability", ADAPT Corporation, 2008
- [9] Rich D. "On-site application of self-compacting concrete (SCC)", Ph.D. thesis, Loughborough University Institutional Repository, 2014.
- [10] ETABS, Ultimate, Version 13.12 Build 1053, Integrated Building Design Software, computer and Structures, Inc., 2013.
- [11] J. Barros, S. Santos, L. Lourenço "Flexural behavior of steel fiber reinforced self-compacting concrete laminar structures", HAC 2008, pp. 1-12.
- [12] Jianxin Ma and Jörg Dietz, " Ultra high performance self-compacting concrete", Dipl.-Ing., Institut für Massivbau und Baustofftechnologie, Universität Leipzig, LACER No. 7, 2002, pp. 33-42.
- [13] International Standard Organization, ISO – 1940, Second edition, 2003.
- [14] Ragab, K.S , "Study punching shear of steel fiber reinforced self-compacting concrete slabs by nonlinear analysis", World Academy of Science, Engineering and Technology, International Journal of Civil, Environmental, Structural, Construction and Architectural Engineering Vol.7, No.9, 2013, pp. 624-635.
- [15] Kaseer, F. M., "Mechanical Properties of Reactive Powder Self Compacting Concrete", M.Sc. Thesis, University of Technology, 2007, pp.5-90.
- [16] Falati, S. "The contribution of non – structural components to the overall dynamic behavior of the concrete floor", PhD thesis, University of Oxford, Hilary, 1999.
- [17] Zaki, S. I., Ragab, K.I, Eisa, A.S., "Flexural behavior of steel fibers reinforced high strength self-compacting concrete slabs", International Journal of Engineering Inventions, Volume 2, Issue 5, March 2013, pp. 01-11.

أداء البلاطات ذات خرسانة المساحيق الفعالة ذاتية الرص تحت الأحمال الديناميكية التوافقية

محمد مكي عباس بلال^{1*} ، صفاء عدنان محمد²

¹ قسم هندسة الطرق والنقل، الجامعة المستنصرية، بغداد، العراق

² قسم هندسة الطرق والنقل، الجامعة المستنصرية، بغداد، العراق

* الباحث الممثل: محمد مكي عباس بلال

نشر في: 31 آذار 2019

الخلاصة – هنالك انواع مختلفة من الأحمال التي يجب أن تؤخذ بنظر الاعتبار في تحليل العناصر الإنشائية وحسب الغاية من المنشأ المقاومة الديناميكية للأحمال للعتبة باستخدام الخرسانة ذات المساحيق الفعالة ذاتية الرص , ضمن محددات وشروط مختلفة والى جانب ذلك تم اجراء الدراسة بوجود الاحمال الساكنة. العتبة الخرسانية المسلحة تم تصميمها تحت الحمل الساكن نسبة لـ ACI-318R-2014 وتم فحص كفاءتها تحت تأثير الحمل الحركي التوافقي. الحمل الساكن ثابت وهي الاحمال الميتة والاحمال الحية نسبة لـ ASCE-07-2010 . تم اجراء تحليل النموذج لايجاد القيمة الذاتية وقيم المتجهات الذاتية وتحليل الخطأ في التردد للعتبة و للتأكد من اداء الخرسانة الاعتيادية والخرسانة ذات المساحيق الفعالة ذاتية الرص تحت الاحمال الثابتة والحركية. التحليل تم بواسطة طريقة العناصر المحددة للبلاطة المسلحة تحت تأثير الأحمال الساكن والديناميكي. النتائج المستخرجة من نتائج التحليل أشارت الى انه عند استخدام الخرسانة ذات المساحيق الفعالة ذاتية الرص كانت نتائج الهطول في البلاطة اقل وكذلك النتائج تأثرت بنوع المسند للبلاطة.